Delta-like ligand 3–targeted radioimmunotherapy for neuroendocrine prostate cancer

Joshua A. Korsen[a,b], Julia A. Gutierrez[a], Kathryn M. Tully[a,b], Lukas M. Carter[a], Zachary V. Samuels[a], Samantha Khitrov[a], John T. Poirier[c], Charles M. Rudin[b,d,e], Yu Chen[d,f], Michael J. Morris[d,g], Lisa Bodei[a], Nagavarakishore Pillarsetty[a,1], and Jason S. Lewis[a,b,e,1]

Neuroendocrine prostate cancer (NEPC) is a lethal subtype of prostate cancer with limited meaningful treatment options. NEPC lesions uniquely express delta-like ligand 3 (DLL3) on their cell surface. Taking advantage of DLL3 overexpression, we developed and evaluated lutetium-177 (^{177}Lu)–labeled DLL3-targeting antibody SC16 (^{177}Lu-DTPA-SC16) as a treatment for NEPC. SC16 was functionalized with DTPA-CHX-A" chelator and radiolabeled with ^{177}Lu to produce ^{177}Lu-DTPA-SC16. Specificity and selectivity of ^{177}Lu-DTPA-SC16 were evaluated in vitro and in vivo using NCI-H660 (NEPC, DLL3-positive) and DU145 (adenocarcinoma, DLL3-negative) cells and xenografts. Dose-dependent treatment efficacy and specificity of ^{177}Lu-DTPA-SC16 radionuclide therapy were evaluated in H660 and DU145 xenograft–bearing mice. Safety of the agent was assessed by monitoring hematologic parameters. ^{177}Lu-DTPA-SC16 showed high tumor uptake and specificity in H660 xenografts, with minimal uptake in DU145 xenografts. At all three tested doses of ^{177}Lu-DTPA-SC16 (4.63, 9.25, and 27.75 MBq/mouse), complete responses were observed in H660-bearing mice; 9.25 and 27.75 MBq/mouse doses were curative. Even the lowest tested dose proved curative in five (63%) of eight mice, and recurring tumors could be successfully re-treated at the same dose to achieve complete responses. In DU145 xenografts, ^{177}Lu-DTPA-SC16 therapy did not inhibit tumor growth. Platelets and hematocrit transiently dropped, reaching nadir at 2 to 3 wk. This was out of range only in the highest-dose cohort and quickly recovered to normal range by week 4. Weight loss was observed only in the highest-dose cohort. Therefore, our data demonstrate that ^{177}Lu-DTPA-SC16 is a potent and safe radioimmunotherapeutic agent for testing in humans with NEPC.

neuroendocrine prostate cancer | radioimmunotherapy | lutetium-177 | DLL3

Androgen receptor (AR) signaling is critical for prostate cancer (PC) cell survival at diagnosis and therefore represents the major therapeutic target for treatment of metastatic disease. Second- and third-generation AR signaling inhibitors (ARSIs; e.g., abiraterone, enzalutamide) have extended the survival of metastatic patients by potent inhibition of AR signaling. Although initially highly effective, androgen blockade is not curative, and acquired resistance can be associated with increased tumor aggressiveness, metastasis, and ultimately death. ARSI treatment can produce tumors that bypass a functional requirement for AR signaling via several mechanisms. In recent years, lineage plasticity has emerged as one of the common mechanisms of resistance that results in the transdifferentiation of AR signaling–dependent PC lesions to AR signaling–independent neuroendocrine PC (NEPC). NEPC bears similarities to small-cell lung cancer (SCLC), including loss of tumor suppressor genes *TP53* and *RB1* and overexpression of the transcriptional factor achaete-scute complex-like 1/achaete-scute homolog 1 (ASCL1) (1, 2). SCLC regimens of platinum doublet chemotherapy have been adopted as current standards of care for NEPC treatment. Unfortunately, the duration of response with these regimens is short, associated with median survival of ∼8.9 mo after histologic transformation to NEPC (3). Therefore, novel therapeutic approaches are needed for treating NEPC patients that can provide durable and meaningful responses.

Delta-like ligand 3 (DLL3) is an inhibitory notch ligand that has emerged as a potential therapeutic target in NEPC (4), SCLC (5), and other cancer types with existing neuroendocrine features (6, 7). DLL3 expression in normal tissues is restricted to intracellular compartments, most notably the Golgi apparatus (8). ASCL1 is a direct transcriptional activator of *DLL3*, leading to aberrant cell surface expression of DLL3. Cell surface DLL3 is not detectable on nonmalignant cells. Although DLL3 is expressed at low densities, the exquisitely selective expression of surface DLL3 on NEPC cells presents a potential target for a variety of therapeutic strategies.

The initial clinical repertoire for DLL3-targeted therapies consists of four agents: (1) the antibody-drug conjugate (ADC) rovalpituzumab-tesirine (RovaT or SC16LD6.5),

Significance

Neuroendocrine prostate cancer (NEPC) is a highly aggressive variant of prostate cancer with few meaningful treatment options. As a result, patients have a poor prognosis once diagnosis is confirmed. NEPC expresses a unique protein called delta-like ligand 3 (DLL3) on the cell surface that is absent on the cell surface of normal cells. Herein, we developed a molecularly targeted radiotherapeutic approach for NEPC treatment using anti-DLL3 antibody SC16 that is radiolabeled with the beta-emitting radioisotope lutetium-177 (^{177}Lu). ^{177}Lu-labeled SC16 demonstrated durable and complete responses in subcutaneous xenograft mouse models of NEPC, with a safe hematologic profile. These data will aid clinical translation and offer a unique avenue for treating NEPC.

[1]To whom correspondence may be addressed. Email: pillarsn@mskcc.org or lewisj2@mskcc.org.

(2) the bispecific T-cell engager AMG757, (3) the chimeric antigen receptor T-cell AMG119, and (4) the trispecific T-cell engager HPN328. First-in-human SCLC studies are currently underway testing AMG757 (NCT03319940), AMG119 (NCT03392064), and HPN328 (NCT04471727). RovaT demonstrated promising preclinical data in treating NEPC (4); however, the ADC was withdrawn from SCLC clinical studies because of unacceptable toxicity attributed to the pyrrolobenzodiazepine (PBD) warhead (9–12). Recently, the anti-DLL3 monoclonal antibody SC16, without the PBD warhead, was redeployed by our laboratory for preclinical imaging. Zirconium-89 ([89]Zr)–radiolabeled SC16 has been successfully synthesized and used as a positron emission tomography (PET) radiopharmaceutical for the noninvasive detection of SCLC (13) and NEPC (14).

NEPC lesions lack expression of prostate-specific membrane antigen (PSMA) (15) and generally express zero or low levels of somatostatin receptors (SSTRs) (16). Therefore, NEPC lesions cannot be efficiently treated with currently available agents such as the PSMA-targeting agent lutetium-177 (^{177}Lu)–labeled PSMA-617 or SSTR2-targeting agent ^{177}Lu-DOTA-TATE. Having demonstrated the ability of [89]Zr-labeled SC16 in imaging DLL3-expressing NEPC xenografts, we sought to explore the potential of ^{177}Lu-labeled SC16 as a targeted radiotherapeutic for the treatment of NEPC. Our most recent work demonstrated the exceptional efficacy of ^{177}Lu-labeled SC16 for the treatment of SCLC in preclinical models (17). Swapping the PET isotope [89]Zr with the β-emitter ^{177}Lu by incorporating the appropriate chelator (CHX-A"-DTPA) allows for delivery of beta-particle radiation in a tumor-specific manner while sparing the surrounding tissue. [177]Lu has a medium decay energy (Eβmax = 497 keV), a maximal tissue penetration of <2 mm, and a half-life of 6.7 d that matches with the half-life of the antibody, making it one of the ideal therapeutic radionuclides. In this work, we describe radiolabeling, in vitro, and in vivo properties of ^{177}Lu-labeled SC16 in targeting DLL3-expressing NEPC tumor xenografts in mouse models and demonstrate dose-dependent treatment responses and establish its safety profile.

Results

^{177}Lu-DTPA-SC16 Characterization and Detection in NEPC Mouse Model.
We used the SC16 antibody as a delivery vehicle for tumor-targeted radionuclide therapy. SC16 was conjugated to the p-SCN-Bn-CHX-A"-DTPA chelator. Under the conditions employed, matrix-assisted laser desorption/ionization time-of-flight mass spectrometry (MALDI-TOF MS) analysis from our laboratory revealed that the average number of DTPA chelates per SC16 antibody was 1.4 ± 0.1 (17). Radiolabeling with ^{177}Lu afforded the radioimmunoconjugate ^{177}Lu-DTPA-SC16 in both high radiochemical yield (≥95%) (SI Appendix, Fig. S1) and high specific activity (0.46 MBq/mg). We previously demonstrated that the radioimmunoconjugate displayed ≥95% stability when incubated in human serum at 37 °C for 7 d (17).

The cell lines chosen for this study were the AR-independent DLL3-positive NEPC H660 cell line and DLL3-negative AR-independent prostate adenocarcinoma DU145 cell line as a negative control. Previous research by our group successfully imaged the DLL3-positive NEPC H660 cell line by PET using [89]Zr-labeled SC16 with the desferrioxamine (DFO) chelator ([89]Zr-DFO-SC16) (14). To confirm that antibody modification with DTPA did not reduce affinity or specificity for target binding, an in vitro cell binding assay was performed in H660 and DU145 cells. ^{177}Lu-DTPA-SC16 still recognized and bound to DLL3 expressed on the cell surface of H660 cells,

with no binding observed in the DLL3-negative DU145 cells (SI Appendix, Fig. S2). DLL3 presence was further verified on resected H660 subcutaneous xenografts by immunohistochemistry. H660 tumors showed high DLL3 staining, which was absent in DU145 subcutaneous xenografts (SI Appendix, Fig. S3A). H660 tumors were also positive for the neuroendocrine marker synaptophysin (SI Appendix, Fig. S3B) but negative for the common PC marker AR (SI Appendix, Fig. S3C).

Ex vivo biodistribution studies with ^{177}Lu-DTPA-SC16 were performed in male nude mice bearing DLL3-positive H660 or DLL3-negative DU145 subcutaneous xenografts. Biodistribution data obtained 24, 72, and 120 h after intravenous administration demonstrated gradually increasing H660 tumor uptake over time, reaching 32.0 ± 4.7 percentage injected dose per gram (%ID/g) at 120 h (Fig. 1A and SI Appendix, Fig. S4). Coadministration of ^{177}Lu-DTPA-SC16 and a 50-fold excess of unlabeled SC16 antibody could significantly reduce tumor uptake, demonstrating specificity of the radioimmunoconjugate to the DLL3 expression in the tumor (Fig. 1A). Our previous work showed low and nonspecific uptake with [89]Zr-labeled isotype-matched IgG in H660 subcutaneous xenografts and was therefore not repeated with ^{177}Lu-labeled IgG, since a change in radioisotope should not significantly alter biodistribution for an intact antibody agent (14). High tumor-to-muscle contrast ratios were also observed (Fig. 1B). In contrast, ^{177}Lu-DTPA-SC16 uptake in the DU145 tumors did not demonstrate a time-dependent increase and was relatively stable over the 120-h time course, reaching 4.5 ± 1.1 %ID/g by 120 h postadministration (Fig. 1C and SI Appendix, Fig. S5). Tumor-to-muscle ratios remained unchanged at all time points (Fig. 1D). This behavior could be expected because of the lack of DLL3 expression.

Organ-level radiation dosimetry estimates were derived from ^{177}Lu-DTPA-SC16 biodistribution data for the H660 xenograft model (SI Appendix, Fig. S6A). Increasing tumor-absorbed dose was observed with increasing dose of ^{177}Lu-DTPA-SC16. The mean tumor-absorbed dose per unit of administered activity was 5.4 Gy/MBq (SI Appendix, Fig. S6B). The critical organ was red bone marrow, which received 1.2 Gy/MBq; all other organs received <500 mGy/MBq.

^{177}Lu-DTPA-SC16 Demonstrates Durable Antitumor Responses.
To investigate the therapeutic potential of ^{177}Lu-labeled SC16 in treating DLL3-expressing NEPC, mice bearing subcutaneous H660 xenografts were randomized into five groups and treated with a single dose of vehicle, increasing single doses of ^{177}Lu-DTPA-SC16 (4.63, 9.25, or 27.75 MBq [125, 250, or 750 μCi]), or a single dose of ^{177}Lu-DTPA-IgG (9.25 MBq). The administered activities were informed by dosimetry calculations derived in non–tumor-bearing mice (17). The 9.25- and 27.75-MBq administered activities were deemed likely to be in the range or upper limit of tolerability with respect to established radiation dose-toxicity thresholds, while plausibly expected to provide tumor control (18, 19). The lowest dose, 4.63 MBq, was chosen as an additional 50% dose reduction from 9.25 MBq to see whether this low dose could still provide measurable therapeutic benefit, while minimizing off-target organ radiotoxicity. Tumor volume was monitored up to 80 d after treatment. Treatment of the H660-bearing mice with 27.75 MBq ^{177}Lu-DTPA-SC16 (~150-Gy tumor-absorbed dose) resulted in complete responses in eight of eight mice, defined as tumor volume <50 mm³ (Fig. 2A and SI Appendix, Fig. S7A for individual tumor growth curves). One of eight mice (mouse 100) experienced a loss of ≥20% pretherapy

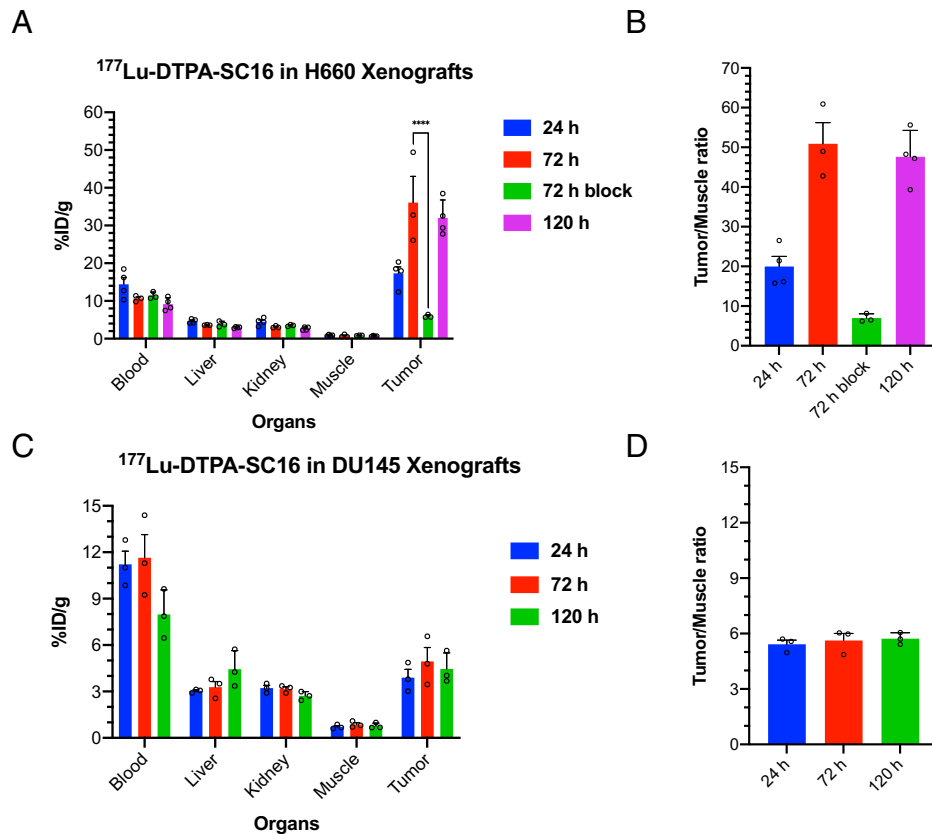**Fig. 1.** Ex vivo biodistribution of ^{177}Lu-DTPA-SC16 in subcutaneous xenograft model of NEPC shows high and selective tumor uptake. (*A*) Select organ biodistribution data at 24, 72, and 120 h postintravenous injection of ^{177}Lu-DTPA-SC16 in athymic male nude mice bearing subcutaneous H660 tumors (*n* = 3–4/cohort). Tumor uptake at 72 h could be blocked with a 50-fold excess of unlabeled SC16 antibody (****P < 0.0001). (*B*) Tumor-to-muscle contrast ratios from the uptake of ^{177}Lu-DTPA-SC16 in H660-bearing mice. (*C*) Select organ biodistribution data at 24, 72, and 120 h postintravenous injection of ^{177}Lu-DTPA-SC16 in athymic male nude mice bearing subcutaneous DU145 tumors (*n* = 3/cohort). (*D*) Tumor-to-muscle contrast ratios from the uptake of ^{177}Lu-DTPA-SC16 in DU145-bearing mice.

weight 17 d posttherapy initiation but demonstrated a complete response by this time (*SI Appendix*, Fig. S8*A*). Two other mice experienced substantial weight loss but rebounded shortly after to pretherapy weights (*SI Appendix*, Fig. S8*A*). Treatment of the H660-bearing mice with 9.25 MBq ^{177}Lu-DTPA-SC16 (∼50-Gy tumor-absorbed dose) similarly resulted in complete responses in eight of eight mice (Fig. 2*A* and *SI Appendix*, Fig. S7*B* for individual tumor growth curves). Mouse 113 required euthanasia because of a corneal ulceration of the left eye, unrelated to therapy, 64 d posttherapy initiation. At time of euthanasia, mouse 113 demonstrated a complete antitumor response. Treatment of the H660-bearing mice with 4.63 MBq ^{177}Lu-DTPA-SC16 (∼25-Gy tumor-absorbed dose) led to complete responses in five of eight mice (Fig. 2*A* and *SI Appendix*, Fig. S7*C* for individual tumor growth curves). These responses were durable in five of eight; in three of eight mice with complete responses, tumor regrowth was noted several weeks posttherapy initiation (time of tumor recurrence: mouse 121, 50 d posttherapy; mouse 122, 75 d posttherapy; mouse 124, 54 d posttherapy). Mouse 127 was found dead 62 d posttherapy. No outward signs of toxicity prior to its death were observed, but therapeutic toxicity could not be ruled out as a possible cause of death. Mouse 127 demonstrated a complete response, which was maintained at the time of death. Mice in the 9.25-MBq ^{177}Lu-DTPA-IgG group demonstrated minimal responses 12 d posttherapy initiation; however, average tumor volume rapidly increased thereafter to 2,000 mm³ (Fig. 2*A* and *SI Appendix*, Fig. S7*D* for individual tumor growth curves). This initial response might be attributable to low-level accumulation of

nontargeted IgG as a result of tumor vascular permeability providing partially effective low-dose beta-irradiation to the tumor. Mice in the saline group all experienced progressive tumor growth without response, as expected (Fig. 2*A* and *SI Appendix*, Fig. S7*E* for individual tumor growth curves). No significant weight loss was observed in the 9.25-MBq ^{177}Lu-DTPA-SC16, 4.63-MBq ^{177}Lu-DTPA-SC16, 9.25-MBq ^{177}Lu-DTPA-IgG, or saline cohorts (*SI Appendix*, Fig. S8 *B–E*). The median survivals for the ^{177}Lu-DTPA-SC16–treated cohorts were not reached at 80 d posttreatment, significantly longer than the 20.5-d median survival for the saline cohort (Fig. 2*B*; P < 0.0001 for 9.25- and 4.63-MBq ^{177}Lu-DTPA-SC16 treatment compared with saline cohort; P = 0.0005 for 27.75-MBq ^{177}Lu-DTPA-SC16 treatment compared with saline cohort). The IgG cohort, with a median survival of 36 d, was only slightly better than the saline cohort (Fig. 2*B*; P = 0.0154).

To further demonstrate that tumor targeting was specific to DLL3 expression in NEPC, mice bearing subcutaneous prostate adenocarcinoma DU145 (DLL3-negative) xenografts were randomized into three groups and treated with a single dose of vehicle, ^{177}Lu-DTPA-SC16 (9.25 MBq), or ^{177}Lu-DTPA-IgG (9.25 MBq). No significant tumor growth inhibition was observed in the treated mice compared with the saline cohort (*SI Appendix*, Figs. S9 and Fig. S10 *A–C* for individual tumor growth curves). Individual tumor graphs in the 9.25-MBq ^{177}Lu-DTPA-SC16 and ^{177}Lu-DTPA-IgG cohorts demonstrated varied tumor responses. A majority of the tumor volumes slowly rose over time, while a select few (e.g., mouse 217) stabilized over the 80-d time course. No significant weight
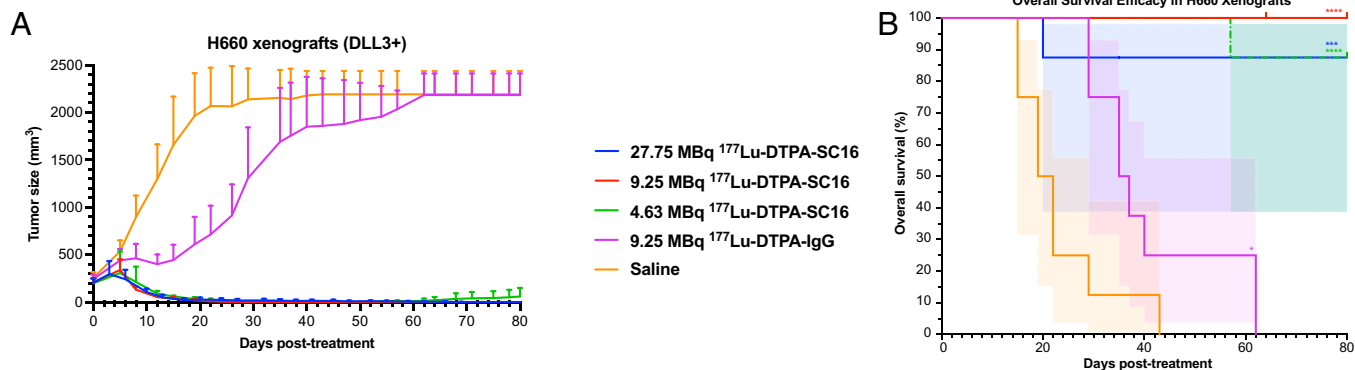
Fig. 2. ^{177}Lu-DTPA-SC16 treatment inhibits tumor growth and extends survival in NEPC-bearing mice. Tumor volume (mm³) growth curves (*A*) and overall survival (%) (*B*) of H660-bearing mice after treatment. Significant tumor growth inhibition was observed in all treated mice compared with saline cohort (*n* = 8/cohort; shading represents 95% confidence interval; *P* = 0.0154, ***P* = 0.0005, ****P* < 0.0001). The red notch at day 64 in the 9.25-MBq ^{177}Lu-DTPA-SC16 cohort refers to mouse 113, which was euthanized unrelated to therapy.

loss was observed in any of these three cohorts (*SI Appendix*, Fig. S11 *A–C*).

^{177}Lu-DTPA-SC16 Treatment Demonstrates Safe Hematologic Profile. Our dosimetry estimates suggested radiogenic toxicity to the hematopoietic marrow to be the predominant dose-limiting toxicity for ^{177}Lu-DTPA-SC16 therapy. To empirically determine if hematologic toxicity would be a concern during DLL3-targeted treatment, a complete blood count profile that measured white blood cells (WBCs), red blood cells (RBCs), and platelets (PLTs) was performed in tumor-bearing mice (both DLL3-positive, H660 and DLL3-negative, DU145 xenografts) prior to therapy initiation followed by weekly blood tests after therapy administration. The pretreatment ranges were calculated as mean ± 1 SD of values collected from the entire cohort of tumor-bearing mice prior to receiving corresponding ^{177}Lu-DTPA-SC16 treatment, designated by gray shading (Fig. 3 *A–C* and *SI Appendix*, Fig. S12 *A–C*). The greatest drop in posttreatment WBC (Fig. 3*A*), RBC (Fig. 3*B*), and PLT (Fig. 3*C*) values was observed in the H660-bearing mice treated with the 27.75-MBq ^{177}Lu-DTPA-SC16 dose. The drop in RBC and PLT values was transient, reaching nadir at 2 to 3 wk with recovery to pretreatment range within 4 wk after therapy initiation. WBC values were slower to recover, gradually increasing after week 3 to slightly below pretherapy range by week 11. Mild petechiae was observed 10 to 13 d postinjection in three of eight mice in the 27.75-MBq cohort, which cleared 15 to 17 d postinjection. A drop in WBCs was observed in the 9.25-MBq ^{177}Lu-DTPA-SC16 cohort but rebounded 3 wk posttreatment (Fig. 3*A*). WBC values were unchanged in the 4.63-MBq ^{177}Lu-DTPA-SC16 cohort after therapy initiation (Fig. 3*A*). No effect on RBCs or PLTs was observed in either the 4.63- or 9.25-MBq ^{177}Lu-DTPA-SC16 cohort (Fig. 3 *B* and *C*). Petechiae were not observed at the 4.63- or 9.25-MBq dose. Overall, negative hematologic effects were absent or mostly mild in the H660-bearing mice, as indicated by a transient drop. In DU145-bearing mice, a drop in WBC count was observed in the 9.25-MBq ^{177}Lu-DTPA-SC16 cohort, which never fully returned to pretherapy values (*SI Appendix*, Fig. S12*A*). The greater observed toxicity in DU145- than in H660-bearing mice might be attributable to DU145 lacking DLL3 expression and therefore not acting as an antigen sink to bind the radiotherapeutic. RBC and PLT values remained unchanged after therapy administration when compared with those before therapy administration (*SI Appendix*, Fig. S12 *B* and *C*).

Repeat Dosing of ^{177}Lu-DTPA-SC16 Leads to Complete Response in Recurring NEPC Tumors. In our lowest radioactive dose treatment group, three of eight mice demonstrated tumor recurrence. We sought to treat these three recurring H660 tumor xenografts (mice 121, 122, and 124) from the 4.63-MBq ^{177}Lu-DTPA-SC16 cohort to determine if a second 4.63-MBq dose would prove beneficial in reinducing tumor response. Fractionated dosing, if effective, is advantageous over single-dose delivery, because it severely reduces nontarget organ toxicity and can be potentially used in patients with cytopenia without complications. To determine whether a second dose would be useful, we first assessed by PET whether DLL3 expression was maintained. In vivo PET imaging with [89]Zr-DFO-SC16 performed 98 d posttherapy initiation demonstrated clear delineation of the recurring H660 tumor xenografts 120 h postadministration of the radioimmunoconjugate (Fig. 4*A*). With DLL3 expression retained, the mice were treated with a second 4.63-MBq ^{177}Lu-DTPA-SC16 dose 100 d following their first dose. Three of the three mice demonstrated rapid responses, as indicated by the abrupt decrease in tumor volume days after administration of the second dose (Fig. 4*B*). Complete responses (tumor volume <50 mm³) were observed 6 d postsecond treatment in mouse 122, 10 d postsecond treatment in mouse 121, and 17 d postsecond treatment in mouse 124. Tumor recurrence was observed once more in the three re-treated mice (time of tumor recurrence: mouse 121, 159 d; mouse 122, 155 d; mouse 124, 147 d); however, a third treatment was not attempted. These data support the potential for lower fractionated doses that may help reduce side effects caused by off-target toxicity or weight loss, which was most prevalent in the 27.75-MBq cohort.

Discussion

NEPC remains a highly lethal disease for which more durably effective therapies are critically needed. These tumors typically lack AR expression and do not depend on AR signaling for growth and are therefore refractory to ARSI-based regimens. The currently recommended treatment for NEPC includes cytotoxic chemotherapy. Although chemotherapy is associated with a high response rate, these responses are transient (<6 mo), and the expected survival is short. A recent phase I/II study explored RovaT as a therapeutic option for DLL3-expressing solid tumors, including NEPC (20). These data included an objective response rate (ORR) of 7% (one of 14) in DLL3-positive NEPC patients receiving a 0.3-mg/kg dose of RovaT. ORR was only 9% (13 of 69) in a pooled group of
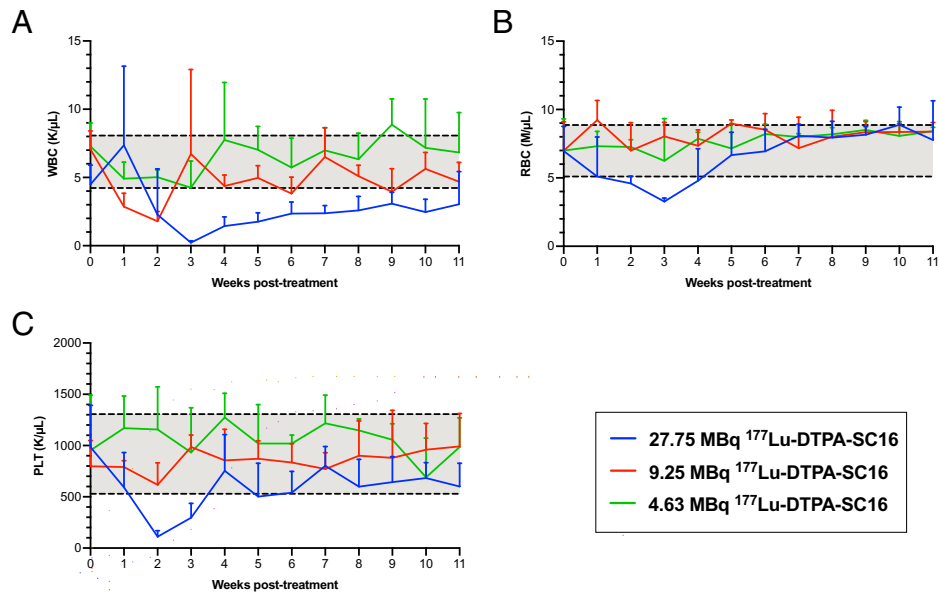
Fig. 3. Hematologic toxicity is either absent or transient in ^{177}Lu-DTPA-SC16–treated mice with NEPC tumors. WBC counts (*A*), RBC counts (*B*), and PLT counts (*C*) in H660-bearing mice that received ^{177}Lu-DTPA-SC16 treatment. Three of the 20 parameters measured are shown. Gray shading indicates the mean ± 1 SD of values collected from the entire cohort of H660-bearing mice prior to therapy initiation (week 0).

patients with other neuroendocrine carcinomas. These disappointing results may be attributable to the dose-limiting toxicities of RovaT, which preclude either higher dose administration or repeat dosing in these patients. There is an unmet need to develop targeted therapies that can provide more durable responses in NEPC patients.

Here we explored a radioimmunotherapeutic approach to treating NEPC employing a ^{177}Lu-labeled DLL3-targeting antibody as a carrier to specifically deliver therapeutic radiation to DLL3-positive tumors. Biodistribution studies of ^{177}Lu-DTPA-SC16 confirmed strong specific uptake in DLL3-positive NEPC H660 tumors. Administration of ^{177}Lu-DTPA-SC16 at 4.63-, 9.25-, and 27.75-MBq doses markedly reduced tumor burden, resulting in complete responses in eight of eight mice in the 9.25- and 27.75-MBq cohorts and five of eight mice in the 4.63-MBq cohort. Weight loss and hematologic toxicity post-therapy initiation were observed only at the highest dose; however, values rebounded ~2 to 4 wk later. DLL3 expression was shown to be maintained by PET in the three recurring H660 tumors in the 4.63-MBq cohort, which originally demonstrated

complete responses. Re-treatment with a second 4.63-MBq dose could once more induce complete responses. Dosimetry estimates showed that the 4.63-MBq dose corresponded to a ~25-Gy tumor-absorbed dose, which is substantially lower than the 50 to 80 Gy required to effectively treat solid cancers and could account for the tumor recurrences observed after the first and second treatments (21). These data suggest a rationale for fractionated DLL3-targeted radioimmunotherapy for patients with DLL3-positive NEPC lesions, which can help overcome the toxicities observed in the highest 27.75-MBq cohort. This is a potentially useful feature in a clinical setting, because NEPC patients are heavily pretreated with chemotherapeutics that commonly result in cytopenia and might not qualify for single high-dose therapy. Fractionation is common clinical practice in radionuclide therapy and external-beam radiotherapy to control tumor growth and decrease organ toxicity.

PC is a highly heterogeneous disease, with multiple distinct tumor foci that can present as an admixture of adenocarcinoma and small-cell neuroendocrine phenotypes. The expression of PSMA can be very heterogeneous, with some metastases expressing
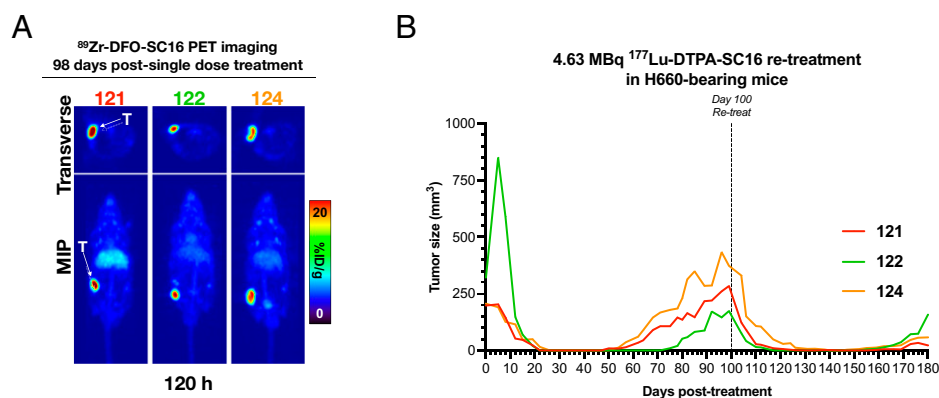

Fig. 4. Re-treatment with ^{177}Lu-DTPA-SC16 reduces tumor growth again in recurring NEPC tumors. (*A*) PET images of ^{89}Zr-DFO-SC16 in H660-bearing mice with recurring tumors. PET images were performed at 120 h postinjection of ^{89}Zr-DFO-SC16, corresponding to 98 d postfirst therapy injection. The images represent maximum intensity projection (MIP) and transverse planar images. See *SI Appendix* for details on PET imaging. (*B*) Individual tumor volume (mm^3) growth curves of H660-bearing mice with recurring tumors. Mice were retreated with a second 4.63-MBq ^{177}Lu-DTPA-SC16 injection 100 d following their first 4.63-MBq ^{177}Lu-DTPA-SC16 injection at day 0.

variable levels of PSMA or being negative altogether. Thus, advanced metastatic castration-resistant prostate cancer (mCRPC) patients treated with ^{177}Lu-labeled PSMA ligands may demonstrate progressive disease despite treatment. DLL3-targeted radioimmunotherapy could serve as a complementary therapy for patients who progress after PSMA-targeted therapy, with these two radioconjugates treating distinct subclonal histologies of this disease.

Together with our prior work, these results demonstrate that [89]Zr-DFO-SC16 and ^{177}Lu-DTPA-SC16 form an effective theranostic (imaging and therapeutic) pair for NEPC patients. PET imaging provides high sensitivity and specificity to assess target expression noninvasively. Each individual lesion can be interrogated, and information about multiple lesions across all anatomical locations can be obtained. [89]Zr-based PET can identify those who are most likely to benefit from targeted radioimmunotherapy with ^{177}Lu-DTPA-SC16. Such an approach has been applied in the phase III VISION trial for the treatment of PSMA-positive mCRPC (NCT03511664) (22). Given the minute quantity of [89]Zr-DFO-SC16 needed for PET imaging, we do not anticipate blocking the therapeutic radioimmunoconjugate from target engagement or therapeutic benefit. A clinical trial of DLL3 PET imaging in SCLC and NEPC patients is currently underway at Memorial Sloan Kettering Cancer (NCT04199741).

Overall, the exceptional response of DLL3-positive NEPC to ^{177}Lu-DTPA-SC16 suggests a potential future treatment to investigate for patients with NEPC. Additional studies are warranted to assess its clinical benefit relative to other available treatment options in NEPC patients. DLL3-targeted radioimmunotherapy can provide a treatment option for patients with a subset of PC that regularly leads to rapid patient decline and death.

In conclusion, in this study, we showed that DLL3-targeted radioimmunotherapy with a ^{177}Lu-labeled DLL3-targeting antibody, SC16, could serve as a potential therapeutic option for investigation in patients with DLL3-positive NEPC.

Materials and Methods

Please refer to the *SI Appendix* for information related to antibody functionalization with CHX-A''-DTPA and radiolabeling (23), biodistribution studies, PET/computed tomography imaging, in vitro cell binding assays, and immunohistochemistry.

Cell Lines and Xenograft Models. H660 and DU145 cell lines were purchased from the American Type Culture Collection and were cultured in aseptic conditions at 37 °C and 5% CO_2 in a humidified atmosphere. H660 was derived from a lymph node metastasis of a 63-y-old patient diagnosed with small-cell NEPC. DU145 was derived from a central nervous system metastasis of a 69-y-old patient with prostate adenocarcinoma. The H660 (DLL3-positive NEPC) cell line was grown in DMEM/F12 supplemented with 10% fetal bovine serum, 10 nM beta-estradiol, 10 nM hydrocortisone, 30 nM sodium selenite, 0.005 mg/mL insulin, 0.01 mg/mL transferrin, 4 mM L-glutamine, 100 units/mL penicillin, and 100 μg/mL streptomycin. The DU145 (DLL3-negative prostate adenocarcinoma) cell line was grown in DMEM supplemented with 10% fetal bovine serum, 100 units/mL penicillin, and 100 μg/mL streptomycin.

All animal experiments performed in this study were approved by the Institutional Animal Care and Use Committee and Research Animal Resource Center at Memorial Sloan Kettering Cancer Center. Six- to 8-wk-old male athymic nude mice (The Jackson Laboratory) were subcutaneously xenografted with 5 million H660 cells or DU145 cells in one-to-one media/matrigel basement membrane matrix (BD Biosciences) on the left flank.

Vernier calipers were used to measure tumor dimensions according to the equation:

$$V = \left(\frac{4\pi}{3}\right) \times \left(\frac{a}{2}\right)^2 \times \frac{b}{2} \qquad [1]$$

V = tumor volume (mm^3)
a = longest axis of tumor (mm)
b = axis perpendicular to longest axis, a (mm)
Assumptions: Tumor volumes were assumed spheroidal.

Tumors were allowed to grow to ∼150 to 300 mm^3 prior to randomization into biodistribution or therapy cohorts ($n = 3$-4, $n = 8$, respectively).

Dosimetry Briefly, for the H660 mouse model, dosimetry estimates were obtained using the MOBY computational mouse phantom (24) in PARaDIM software (25). For the purposes of dosimetry, the measured uptake in the blood was assumed to be representative of red bone marrow, and the uptake in the muscle tissue was assumed to be representative of any remaining organs not harvested during the biodistribution studies (i.e., not listed in *SI Appendix*, Fig. S4). For each organ i, the organ uptake values quantified in the percentage of injected activity per gram of tissue as a function of time, $(\%ID/g)_i(t)$, were reexpressed as standardized uptake values normalized by total body weight (SUV_{bw}) at each time point:

$$SUV_{bw,i}(t) = \left[\frac{\%ID}{g}\right]_i(t) \times \frac{m_{mouse}}{100\%} \qquad [2]$$

m_{mouse} = mouse total body mass (g)

The 25-g MOBY mouse phantom was assumed to be representative of the H660 cohort, such that at each time point, the standardized uptake value in phantom organ I, $SUV_{bw,I}$, was equal to the mean $SUV_{bw,i}$. Time-activity curves for each of the phantom organs were then obtained using the following equation:

$$FID_I(t) = SUV_{bw,I}(t) \times \frac{m_I}{m_{phantom}} \times e^{-\lambda_p t} \qquad [3]$$

FID_I = fraction of administered activity in phantom organ I
m_I = mass of phantom organ I (g)
$m_{phantom}$ = phantom total mass (g)
λ_p = [177]Lu physical decay constant

Note that FID_I in Eq. 3 represents effective clearance (as opposed to biologic clearance) and is not corrected for decay back to time of administration, as is the case for the SUV or %ID/g. For most phantom organs, the effective time-activity curves were well described by a monophasic exponential decay function of the following form:

$$FID_I(t) = Ae^{-(\lambda_p + \lambda_b)t} \qquad [4]$$

Therefore, Eq. 4 was fit to each organ time-activity curve via the least-squares method. For each of these organs, the time-integrated activity coefficient, $\tilde{a}_I$ (h), was determined from the analytic expression for the integral of Eq. 4 over time interval (0, ∞). The time-activity curve for the tumor was not well described by a monoexponential decay function, so the trapezoidal method was used; for the tumor, beyond the last measured time point, the clearance was assumed to occur via physical decay only. Finally, the time-integrated activity coefficients were input into PARaDIM to compute the absorbed dose coefficients (mGy/MBq); in PARaDIM, 1.5×10^7 particle histories were simulated using the default parameters.

In Vivo Therapy in Subcutaneous Xenograft Models. Mouse tumor volumes, weights, and blood samples (collected via retro-orbital blood draw) were measured pretherapy followed by mouse randomization into one of five therapy cohorts for H660-bearing mice and one of three therapy cohorts for DU145-bearing mice ($n = 8$ mice per group). After randomization, mice were injected with vehicle (0.9% sterile saline, 150 μL via intravenous tail vein injection) or radioimmunoconjugate (4.63, 9.25, or 27.75 MBq ^{177}Lu-DTPA-SC16 or 9.25 MBq ^{177}Lu-DTPA-IgG; 60 μg monoclonal antibody [mAb]/injection; 150 μL via intravenous tail vein injection). Following therapy initiation, tumor volumes and weights were measured twice weekly for 80 d or until mice reached a defined end point: (1) tumor volume ≥2,000 mm^3, (2) ≥20% pretherapy weight loss, (3) or severe petechiae. Blood samples were collected once a week and analyzed using an Element HT5 (Heska Corporation) to measure potential hematologic toxicity. For the re-treatment in the 4.63-MBq ^{177}Lu-DTPA-SC16 cohort, the three recurring H660 tumor-bearing mice were injected with a second dose of ^{177}Lu-DTPA-SC16 (4.63 MBq; 60 μg mAb/injection; 150 μL via intravenous tail vein injection) 100 d after administration of the first dose. Following

therapy initiation, tumor volumes were measured twice weekly for 80 d or until mice reached the defined end points mentioned earlier.

Statistical Analyses. All data presented are expressed as mean ± SD and were analyzed using GraphPad Prism 8 software. Two-way ANOVA test with a threshold for statistical significance set at $P < 0.05$ was used to evaluate the blocking study in the subcutaneous xenograft. A correction for multiple comparisons was performed using the Holm-Sidak method to determine statistical significance ($\alpha = 0.05$). Data for the in vitro cell binding assay were analyzed by unpaired two-tailed t test using GraphPad Prism 8 software with a threshold for statistical significance set at $P < 0.05$. Kaplan-Meier survival curves and a log-rank test (Mantel-Cox) were used to evaluate the survival of mice between cohorts.

Data Availability. All study data are included in the article and/or supporting information.

Author affiliations: [a]Department of Radiology, Memorial Sloan Kettering Cancer Center, New York, NY 10065; [b]Department of Pharmacology, Weill Cornell Medicine, New York, NY 10021; [c]Perlmutter Cancer Center, New York University Langone Health, New York, NY 10016; [d]Department of Medicine, Memorial Sloan Kettering Cancer Center, New York, NY 10065; [e]Molecular Pharmacology Program, Memorial Sloan Kettering Cancer Center, New York, NY 10065; [f]Human Oncology and Pathogenesis Program, Memorial Sloan Kettering Cancer Center, New York, NY 10065; and [g]Department of Medicine, Weill Cornell Medicine, New York, NY 10021

1. M. D. Borromeo et al., ASCL1 and NEUROD1 reveal heterogeneity in pulmonary neuroendocrine tumors and regulate distinct genetic programs. Cell Rep. **16**, 1259–1272 (2016).
2. S. Y. Ku et al., Rb1 and Trp53 cooperate to suppress prostate cancer lineage plasticity, metastasis, and antiandrogen resistance. Science **355**, 78–83 (2017).
3. V. Conteduca et al., Clinical features of neuroendocrine prostate cancer. Eur. J. Cancer **121**, 7–18 (2019).
4. L. Puca et al., Delta-like protein 3 expression and therapeutic targeting in neuroendocrine prostate cancer. Sci. Transl. Med. **11**, eaav0891 (2019).
5. L. R. Saunders et al., A DLL3-targeted antibody-drug conjugate eradicates high-grade pulmonary neuroendocrine tumor-initiating cells in vivo. Sci. Transl. Med. **7**, 302ra136 (2015).
6. V. S. Koshkin et al., Transcriptomic and protein analysis of small-cell bladder cancer (SCBC) identifies prognostic biomarkers and DLL3 as a relevant therapeutic target. Clin. Cancer Res. **25**, 210–221 (2019).
7. X. Ding, F. Li, L. Zhang, Knockdown of Delta-like 3 restricts lipopolysaccharide-induced inflammation, migration and invasion of A2058 melanoma cells via blocking Twist1-mediated epithelial-mesenchymal transition. Life Sci. **226**, 149–155 (2019).
8. I. Geffers et al., Divergent functions and distinct localization of the Notch ligands DLL1 and DLL3 in vivo. J. Cell Biol. **178**, 465–476 (2007).
9. M. L. Johnson et al., Rovalpituzumab tesirine as a maintenance therapy after first-line platinum-based chemotherapy in patients with extensive-stage-SCLC: Results from the phase 3 MERU study. J. Thorac. Oncol. **16**, 1570–1581 (2021).
10. F. Blackhall et al., Efficacy and safety of rovalpituzumab tesirine compared with topotecan as second-line therapy in DLL3-high SCLC: Results from the phase 3 TAHOE study. J. Thorac. Oncol. **16**, 1547–1558 (2021).
11. D. Morgensztern et al., Efficacy and safety of rovalpituzumab tesirine in third-line and beyond patients with DLL3-expressing, relapsed/refractory small-cell lung cancer: Results from the phase II TRINITY study. Clin. Cancer Res. **25**, 6958–6966 (2019).
12. J. T. Poirier et al., New approaches to SCLC therapy: From the laboratory to the clinic. J. Thorac. Oncol. **15**, 520–540 (2020).
13. S. K. Sharma et al., Noninvasive interrogation of DLL3 expression in metastatic small cell lung cancer. Cancer Res. **77**, 3931–3941 (2017).
14. J. A. Korsen et al., Molecular imaging of Neuroendocrine Prostate Cancer by targeting Delta-like Ligand 3. J. Nucl. Med, 10.2967/jnumed.121.263221 (2022).
15. H. Beltran, F. Demichelis, Therapy considerations in neuroendocrine prostate cancer: What next? Endocr. Relat. Cancer **28**, T67–T78 (2021).
16. C. Werner et al., Evaluation of somatostatin and CXCR4 receptor expression in a large set of prostate cancer samples using tissue microarrays and well-characterized monoclonal antibodies. Transl. Oncol. **13**, 100801 (2020).
17. K. M. Tully et al., Radioimmunotherapy targeting delta-like ligand 3 in small cell lung cancer exhibits antitumor efficacy with low toxicity. Clin. Cancer Res. **28**, 1391–1401 (2022).
18. B. Emami et al., Tolerance of normal tissue to therapeutic irradiation. Int. J. Radiat. Oncol. Biol. Phys. **21**, 109–122 (1991).
19. S. M. Larson, J. A. Carrasquillo, N. K. Cheung, O. W. Press, Radioimmunotherapy of human tumours. Nat. Rev. Cancer **15**, 347–360 (2015).
20. A. S. Mansfield et al., A phase I/II study of rovalpituzumab tesirine in delta-like 3-expressing advanced solid tumors. NPJ Precis. Oncol. **5**, 74 (2021).
21. G. Sgouros, L. Bodei, M. R. McDevitt, J. R. Nedrow, Radiopharmaceutical therapy in cancer: Clinical advances and challenges. Nat. Rev. Drug Discov. **19**, 589–608 (2020).
22. O. Sartor et al.; VISION Investigators, Lutetium-177-PSMA-617 for metastatic castration-resistant prostate cancer. N. Engl. J. Med. **385**, 1091–1103 (2021).
23. J. P. Holland, Y. Sheh, J. S. Lewis, Standardized methods for the production of high specific-activity zirconium-89. Nucl. Med. Biol. **36**, 729–739 (2009).
24. M. A. Keenan, M. G. Stabin, W. P. Segars, M. J. Fernald, RADAR realistic animal model series for dose assessment. J. Nucl. Med. **51**, 471–476 (2010).
25. L. M. Carter et al., PARaDIM: A PHITS-based Monte Carlo tool for internal dosimetry with tetrahedral mesh computational phantoms. J. Nucl. Med. **60**, 1802–1811 (2019).